Mitogen-activated protein kinase kinase 1/2 inhibitors and 17-allylamino-17-demethoxygeldanamycin synergize to kill human gastrointestinal tumor cells *in vitro* via suppression of c-FLIP-s levels and activation of CD95

Margaret A. Park,[1] Guo Zhang,[1] Clint Mitchell,[1] Mohamed Rahmani,[2] Hossein Hamed,[1] Michael P. Hagan,[3] Adly Yacoub,[1,3] David T. Curiel,[5] Paul B. Fisher,[4] Steven Grant,[1,2] and Paul Dent[1,3]

Departments of [1]Biochemistry and Molecular Biology, [2]Medicine, [3]Radiation Oncology, and [4]Human Genetics and Molecular Genetics, Virginia Commonwealth University, Richmond, Virginia and [5]Division of Human Gene Therapy, Departments of Medicine, Pathology and Surgery, and Gene Therapy Center, University of Alabama at Birmingham, Birmingham, Alabama

Abstract

Prior studies have noted that inhibitors of mitogen-activated protein kinase (MAPK) kinase 1/2 (MEK1/2) enhanced geldanamycin lethality in malignant hematopoietic cells by promoting mitochondrial dysfunction. The present studies focused on defining the mechanism(s) by which these agents altered survival in carcinoma cells. MEK1/2 inhibitors [PD184352; AZD6244 (ARRY-142886)] interacted in a synergistic manner with geldanamycins [17-allylamino-17-demethoxygeldanamycin (17AAG) and 17-dimethylaminoethylamino-17-demethoxy-geldanamycin] to kill hepatoma and pancreatic carcinoma cells that correlated with inactivation of extracellular signal-regulated kinase 1/2 and AKT and with activation of p38 MAPK; p38 MAPK activation was reactive oxygen species dependent. Treatment of cells with MEK1/2 inhibitors and 17AAG reduced expression of c-FLIP-s that was mechanistically connected to loss of MEK1/2 and AKT function; inhibition of caspase-8 or overexpression of c-FLIP-s abolished cell killing by MEK1/2 inhibitors and 17AAG. Treatment of cells with MEK1/2 inhibitors and 17AAG caused a p38 MAPK-dependent plasma membrane clustering of CD95 without altering the levels or cleavage of FAS ligand. In parallel, treatment of cells with MEK1/2 inhibitors and 17AAG caused a p38 MAPK-dependent association of caspase-8 with CD95. Inhibition of p38 MAPK or knockdown of BID, FAS-associated death domain, or CD95 expression suppressed MEK1/2 inhibitor and 17AAG lethality. Similar correlative data were obtained using a xenograft flank tumor model system. Our data show that treatment of tumor cells with MEK1/2 inhibitors and 17AAG induces activation of the extrinsic pathway and that suppression of c-FLIP-s expression is crucial in transduction of the apoptotic signal from CD95 to promote cell death. [Mol Cancer Ther 2008;7(9):2633–48]

Received 4/24/08; revised 6/9/08; accepted 6/9/08.

Grant support: USPHS grants R01-DK52825, P01-CA104177, and R01-CA108325 and The Jim Valvano ''V'' Foundation (P. Dent); USPHS grants R01-CA63753 and R01-CA77141 and Leukemia Society of America grant 6405-97 (S. Grant); USPHS grants P01-CA104177, R01-CA097318, R01-CA098172, and P01-NS031492 and The Samuel Waxman Cancer Research Foundation (P.B. Fisher); and USPHS grant P01-CA104177 (D.T. Curiel). P. Dent is The Universal, Inc., Professor in Signal Transduction Research and P.B. Fisher is a Samuel Waxman Cancer Research Foundation investigator.

The costs of publication of this article were defrayed in part by the payment of page charges. This article must therefore be hereby marked *advertisement* in accordance with 18 U.S.C. Section 1734 solely to indicate this fact.

Note: M.A. Park and G. Zhang contributed equally to the execution and completion of these studies.

Requests for reprints: Paul Dent, Department of Biochemistry and Molecular Biology, Virginia Commonwealth University, 401 College Street, Massey Cancer Center, Box 980035, Richmond, VA 23298-0035. Phone: 804-628-0861; Fax: 804-827-1309. E-mail: pdent@vcu.edu

doi:10.1158/1535-7163.MCT-08-0400

Introduction

In the United States, hepatoma is diagnosed in ~19,000 patients per annum with ~17,000 deaths from the disease, with a 5-year survival rate of <10%. Hepatoma is a leading cause of diagnosed cancer in Africa and Asia and represents the fifth most commonly diagnosed malignancy in the world (1). In the United States, pancreatic cancer is diagnosed in ~37,000 patients per annum with ~34,000 deaths every year (2). Pancreatic cancer has a 5-year survival rate of <5%. These statistics emphasize the need to develop novel therapies against these lethal malignancies.

The Raf/mitogen-activated protein kinase (MAPK) kinase 1/2 (MEK1/2)/extracellular signal-regulated kinase 1/2 (ERK1/2) pathway is frequently dysregulated in neoplastic transformation, including hepatocellular carcinoma (3). The MEK1/2-ERK1/2 module comprises, along with c-Jun NH_2-terminal kinase (JNK1/2) and p38 MAPK, members of the MAPK superfamily (4, 5). These kinases are involved in responses to diverse mitogens and environmental stresses, including DNA damage, osmotic stress, and hypoxia, and have also been implicated in multiple cellular functions, including proliferation, differentiation, and cell survival processes. Although exceptions exist, activation of the ERK1/2 pathway is generally associated with cell survival, whereas induction of JNK1/2 and p38 MAPK pathways generally signals apoptosis. There is also evidence that the net balance of signals in terms of amplitude and duration between the cytoprotective ERK1/2 and the stress-related JNK1/2 and p38 MAPK

pathways determines whether a cell lives or dies following various insults. Although the mechanism(s) by which ERK1/2 activation promotes survival is not known with certainty, several downstream antiapoptotic effector proteins have been identified, including direct inactivation of proapoptotic proteins such as caspase-9, BAD, and BIM and increased expression of antiapoptotic proteins such as BCL-XL, MCL-1, and c-FLIP proteins (6–11). In view of the importance of the MEK1/2-ERK1/2 pathway in neoplastic cell survival, MEK1/2 inhibitors have been developed by several pharmaceutical companies and have entered clinical trials, including PD184352 (CI-1040), the second-generation Pfizer MEK1/2 inhibitor PD 0325901, and the AstraZeneca drug AZD6244 (ARRY-142886; refs. 12, 13).

Heat shock protein 90 (HSP90) is a chaperone protein involved in the proper folding and intracellular disposition of multiple proteins involved in cell signaling and survival (14, 15). Tumor cells generally have higher rates of protein synthesis than nonneoplastic cells, and disruption of HSP90 function in tumor cells (e.g., by benzoquinoid ansamycin antibiotics such as geldanamycin; ref. 16) has been shown to induce improper folding of diverse proteins, including Raf-1, B-Raf, AKT, ERBB family receptors, among numerous others, culminating in their proteasomal degradation (17). These events have been shown to induce apoptosis or, alternatively, to increase the susceptibility of tumor cells to established cytotoxic agents (18, 19). Such considerations have led to the development of clinically relevant HSP90 antagonists, such as 17-allylamino-17-demethoxygeldanamycin (17AAG), which has both superior pharmacokinetic and reduced normal tissue toxicity characteristics compared with geldanamycin (20, 21). Many studies have argued that inhibition of the phosphatidylinositol 3-kinase/AKT pathway, rather than the Raf-MEK1/2-ERK1/2 pathway, represents a key component of 17AAG toxicity and sensitization effects in tumor cells (22–27). Free plasma concentrations of 17AAG in patients have been noted to be in the low 1 to 5 μmol/L range for up to 12 h after drug infusion, which is significantly higher than the required concentration of drug to inhibit HSP90 function (25, 26).

The goal of the present studies was to determine whether, and by what mechanism(s), clinically relevant MEK1/2 inhibitors might enhance the activity of clinically relevant geldanamycins [17AAG and 17-dimethylaminoethylamino-17-demethoxy-geldanamycin (17DMAG)] against human hepatoma and other gastrointestinal and genitourinary tumor cells *in vitro* and *in vivo*. Our results indicate that clinically relevant MEK1/2 inhibitors interact synergistically with 17AAG and 17DMAG to induce CD95 (FAS receptor)–dependent cell death.

Materials and Methods

Materials

Total BAX, cleaved caspase-3, phosphorylated/total ERK1/2/5, phosphorylated/total JNK1-3, phosphorylated/total p38 MAPK, anti-S473 AKT, and total AKT antibodies were purchased from Cell Signaling Technologies. Active BAX specific antibody (6A7) for immunoprecipitation was purchased from Sigma. The c-FLIP-s/L and all the secondary antibodies (anti-rabbit, anti-mouse, and anti-goat horseradish peroxidase) were purchased from Santa Cruz Biotechnology. The JNK inhibitor peptide, caspase inhibitors (zVAD, IETD, and LEHD), and 17AAG was supplied by Calbiochem as powder, dissolved in sterile DMSO, and stored frozen under light-protected conditions at −80°C. Enhanced chemiluminescence kits were purchased from Amersham Enhanced Chemiluminescence System and NEN Life Science Products (NEN Life Science Products). Trypsin-EDTA, RPMI, and penicillin-streptomycin were purchased from Life Technologies. BAX/BAK-/-, BIM-/-, and BID-/- fibroblasts were kindly provided by Dr. S. Korsmeyer (Harvard University). HuH7, HEPG2 and HEP3B (hepatoma), pancreatic (PANC1 and Mia Paca2), colorectal (SW480 and HCT116), and prostate (DU145 and PC3) cancer cells were obtained from the American Type Culture Collection. Commercially available validated short hairpin RNA molecules to knockdown RNA/protein levels were from Qiagen: CD95 (SI02654463; SI03118255), FAS-associated death domain (FADD; SI00300223; SI03648911), and BID (SI02654568; SI02661911). The dominant-negative p38 MAPK and activated MEK1 EE recombinant adenoviruses were kindly provided by Dr. K. Valerie (Virginia Commonwealth University) and Dr. J. Moltken (University of Cincinnati), respectively. The proprietary drug 17DMAG was supplied by the Dr. David Gius (Radiation Oncology Branch, Radiation Oncology Sciences Program, National Cancer Institute, NIH). Other reagents were of the highest quality commercially available (11, 27, 28).

Methods

Cell Culture and *In vitro* Exposure of Cells to Drugs. All established cell lines were cultured at 37°C [5% (v/v) CO_2] *in vitro* using RPMI supplemented with 5% (v/v) FCS and 10% (v/v) nonessential amino acids. For short-term cell killing assays and immunoblotting, cells were plated at a density of 3×10^3 per cm^2 and 36 h after plating were treated with various drugs as indicated. *In vitro* small-molecule inhibitor treatments were from a 100 mmol/L stock solution of each drug and the maximal concentration of vehicle (DMSO) in medium was 0.02% (v/v). For adenoviral infection, cells were infected 12 h after plating and the expression of the recombinant viral transgene was allowed to occur for 24 h before any additional experimental procedure. Cells were not cultured in reduced serum medium during any study.

Cell Treatments, SDS-PAGE, and Western Blot Analysis. Unless otherwise indicated in the figure legend, cells were treated with either vehicle (DMSO) or the combination of MEK1/2 inhibitor PD184352 (1 μmol/L) or PD98059 (20 μmol/L) as indicated and geldanamycin (1 μmol/L 17AAG or 0.25 μmol/L 17DMAG) or both agents combined. For SDS-PAGE and immunoblotting, cells were lysed in either a nondenaturing lysis buffer and prepared for immunoprecipitation as described in refs. 27, 28 or in whole-cell lysis buffer [0.5 mol/L Tris-HCl (pH 6.8), 2% SDS, 10% glycerol, 1% β-mercaptoethanol, and 0.02% bromophenol blue], and the samples were boiled for 30

min. After immunoprecipitation, samples were boiled in whole-cell lysis buffer. The boiled samples were loaded onto 10% to 14% SDS-PAGE and electrophoresis was run overnight. Proteins were electrophoretically transferred onto 0.22 μm nitrocellulose and immunoblotted with indicated primary antibodies against the different proteins. All immunoblots were visualized by enhanced chemiluminescence. For presentation, immunoblots were digitally scanned at 600 dpi using Adobe Photoshop CS2, their colors were removed, and figures were generated in Microsoft PowerPoint. Densitometric analysis for enhanced chemiluminescence immunoblots was done using a Fluorochem 8800 Image System and the respective software (Alpha Innotech) and band densities were normalized to that of a total protein loading control.

Recombinant Adenoviral Vectors; Infection *In vitro*. We generated and purchased previously noted recombinant adenoviruses to express constitutively activated and dominant-negative AKT and MEK1 proteins, dominant-negative caspase-9, the caspase-9 inhibitor XIAP, the endogenous caspase-8 inhibitor c-FLIP-s, the polyoma virus caspase-8 inhibitor CRM A, and the mitochondrial protective protein BCL-XL (Vector Biolabs; ref. 27). Unless otherwise stated, cells were infected with these adenoviruses at an approximate multiplicity of infection of 50. As noted above, cells were further incubated for 24 h to ensure adequate expression of transduced gene products before drug exposures.

Small Interfering RNA Transfection *In vitro*. A defined prevalidated small interfering RNA (siRNA; ~10 nmol/L; Ambion Technologies) was diluted into 50 μL growth medium lacking fetal bovine serum (FBS) and penicillin-streptomycin. Based on the manufacturer's instructions, an appropriate amount of LipofectAMINE 2000 reagent (usually 1 μL; Invitrogen) was diluted into a separate vial containing medium with lacking FBS or penicillin-streptomycin. The two solutions were incubated separately at room temperature for 5 min and then mixed together (vortexed) and incubated at room temperature for 30 min. The mixture was added to each well (slide or 12-well plate) containing an appropriate amount (~0.5 mL) of penicillin-streptomycin- and FBS-free medium. Cells were incubated for 2 to 4 h at 37°C with gentle rocking. Medium was then replaced with 1 mL of 1× penicillin-streptomycin- and FBS-containing medium.

Plasmid Transfection. Plasmid DNA (0.5 μg/total plasmid transfected) was diluted into 50 μL RPMI that lacked supplementation with FBS or penicillin-streptomycin. LipofectAMINE 2000 reagent (1 μL; Invitrogen) was diluted into 50 μL growth medium that lacked supplementation with FBS or penicillin-streptomycin. The two solutions were then mixed together and incubated at room temperature for 30 min. The total mix was added to each well (4-well glass slide or 12-well plate) containing 200 μL growth medium that lacked supplementation with FBS or penicillin-streptomycin. The cells were incubated for 4 h at 37°C, after which time the medium was replaced with RPMI containing 5% (v/v) FBS and 1× penicillin-streptomycin (27, 28).

Detection of Cell Death by Trypan Blue, Hoechst, Terminal Deoxynucleotidyl Transferase–Mediated dUTP Nick End Labeling, and Flow Cytometric Assays. Cells were harvested by trypsinization with trypsin/EDTA for ~10 min at 37°C. As some apoptotic cells detached from the culture substratum into the medium, these cells were also collected by centrifugation of the medium at 1,500 rpm for 5 min. The pooled cell pellets were resuspended and mixed with trypan blue dye. Trypan blue stain, in which blue dye–incorporating cells were scored as being dead, was done by counting of cells using a light microscope and a hemacytometer. Five hundred cells from randomly chosen fields were counted and the number of dead cells was counted and expressed as a percentage of the total number of cells counted. For confirmatory purposes, the extent of apoptosis was evaluated by assessing Hoechst and terminal deoxynucleotidyl transferase–mediated dUTP nick end labeling–stained cytospin slides under fluorescent light microscopy and scoring the number of cells exhibiting the ''classic'' morphologic features of apoptosis and necrosis. For each condition, 10 randomly selected fields per slide were evaluated, encompassing at least 1,500 cells. Alternatively, the Annexin V/propidium iodide assay was carried to determine cell viability out as per the manufacturer's instructions (BD PharMingen) using a Becton Dickinson FACScan flow cytometer (27, 28).

***In vivo* Exposure of HEP3B Tumors to Drugs.** Athymic female NCr-*nu/nu* mice were obtained from The Jackson Laboratory. Mice were maintained under pathogen-free conditions in facilities approved by the American Association for Accreditation of Laboratory Animal Care and in accordance with current regulations and standards of the U.S. Department of Agriculture, the U.S. Department of Health and Human Services, and the NIH. HEP3B cells were cultured and isolated by trypsinization followed by cell number determination using a hemacytometer. Cells were resuspended in PBS and 10 million tumor cells per 100 μL PBS were injected into the right rear flank of each mouse, and tumors were permitted to form to a volume of ~100 mm^3 over the following 3 to 4 weeks. PD184352 was prepared and administered i.p. three times daily as described in Hawkins et al. (6). The geldanamycin 17AAG was prepared in an identical manner to PD184352 and administered once daily. Both agents were dosed at 25 mg/kg for 30 h.

***Ex vivo* Manipulation of Carcinoma Tumors.** Animals were euthanized by CO_2 and placed in a BL2 cell culture hood on a sterile barrier mat. The bodies of the mice were soaked with 70% (v/v) ethanol and the skin around the tumor was removed using small scissors, forceps, and a disposable scalpel. These implements were flame sterilized between removal of the outer and inner layers of skin. A piece of the tumor (~50% by volume) was removed and placed in a 10 cm dish containing 5 mL RPMI on ice. In parallel, the remainder of the tumor was placed in 5 mL Streck Tissue Fixative (Fisher Scientific) in a 50 mL conical tube for H&E fixation. The tumor sample that had been placed in RPMI was minced with a sterile disposable

scalpel into the smallest possible pieces and then placed in a sterile disposable flask. The dish was rinsed with 6.5 mL RPMI, which was then added to the flask. A 10× solution of collagenase (Sigma; 2.5 mL, 28 units/mL final concentration) and 10× enzyme mixture containing DNase (Sigma; 308 units/mL final concentration) and Pronase (EMD Sciences; 22,500 units/mL final concentration) in a volume of 1 mL were added to the flask. The flasks were placed into an orbital shaking incubator at 37°C for 1.5 h at 150 rpm. Following digestion, the solution was passed through a 0.4 μm filter into a 50 mL conical tube. After mixing, a sample was removed for viable and total cell counting using a hemacytometer. Cells were centrifuged at $500 \times g$ for 4 min, the supernatant was removed, and fresh RPMI containing 10% (v/v) FCS was added to give a final resuspended cell concentration of 1×10^6 cells/mL. Cells were diluted and plated in 10 cm dishes in triplicate at a concentration of 2×10^3 per dish for control and 4×10^3 per dish for all other drug exposures.

Immunohistochemistry and Staining of Fixed Tumor Sections. Fixed tumors were embedded in paraffin wax and 10 μm slices were obtained using a microtone. Tumor sections were deparaffinized and rehydrated, and antigen was retrieved in a 10 mmol/L (w/v) sodium citrate/citric acid buffer (pH 6.7) heated to 90°C in a constant temperature microwave oven. Prepared sections were then blocked and subjected to immunohistochemistry as per the instructions of the manufacturer for each primary antibody [P-AKT (S473), P-p38, P-ERK1/2, cleaved caspase-3, and c-FLIP-s]. The permanently mounted slides were allowed to dry overnight and were photographed at the indicated magnification. The area selected for all photomicrographs was the proliferative zone, within 2 mm of, or juxtaposed to leading edge of the tumor.

Preparation of S-100 Fractions and Assessment of Cytochrome c Release. Cells were harvested after GST-MDA-7 treatment by centrifugation at 600 rpm for 10 min at 4°C and washed in PBS. Cells ($\sim 1 \times 10^6$) were lysed by incubation for 3 min in 100 μL lysis buffer containing 75 mmol/L NaCl, 8 mmol/L Na_2HPO_4, 1 mmol/L NaH_2PO_4, 1 mmol/L EDTA, and 350 μg/mL digitonin. The lysates were centrifuged at 12,000 rpm for 5 min, and the supernatant was collected and added to an equal volume of 2× Laemmli buffer. The protein samples were quantified and separated by 15% SDS-PAGE (27, 28).

Data Analysis. Comparison of the effects of various treatments was done using one-way ANOVA and a two tailed Student's t test. Differences with $P < 0.05$ were considered statistically significant. These values were determined using the statistical programming within SigmaStat and SigmaPlot. Median dose-effect isobologram analyses to determine synergism of drug interaction were done according to the methods of Chou and Talalay using the Calcusyn program for Windows (BioSoft). A combination index value < 1.00 indicates synergy of interaction between the drugs; a value of 1.00 indicates additivity; a value of >1.00 equates to antagonism of action between the agents. Data points from all experiments are the mean of multiple individual data points summated from the stated number of multiple experiments (mean data = Σn, all data points, ± SE; refs. 27, 28).

Results

MEK1/2 Inhibitors and Geldanamycins Interact to Kill Hepatoma Cells in a Synergistic Fashion *In vitro*

Initial experiments focused on the regulation of hepatoma and pancreatic carcinoma cell survival following exposure to MEK1/2 inhibitors [PD184352 (CI-1040) and AZD6244 (ARRY-142886)] and the geldanamycin 17AAG. Treatment of HuH7, HEPG2, and HEP3B (hepatoma) cells with 17AAG and PD184352 caused a greater than additive induction of cell killing than either individual agent alone within 48 h of exposure as judged in terminal deoxynucleotidyl transferase–mediated dUTP nick end labeling, trypan blue, and Annexin V/propidium iodide flow cytometry assays (Fig. 1A and *B*). Similar data to that with PD184352 were obtained when the MEK1/2 inhibitor AZD6244 was used (Supplementary Fig. S1).[6] Similar hepatoma cell killing data to that obtained with 17AAG were generated when the HSP90 inhibitor 17DMAG was used in combination with the MEK1/2 inhibitor PD184352; cell killing was blocked by the small-molecule caspase-8 inhibitor IETD (Fig. 1C) (see also data in ref. 28). Using median dose-effect analyses, we determined using short-term cell death and long-term colony formation assays whether MEK1/2 inhibitors and 17AAG interacted in a synergistic manner: both PD184352 and AZD6244 enhanced 17AAG lethality in a synergistic manner with combination index values of <1.00 (Fig. 1D; data not shown). Similar cell killing data to that generated in hepatoma cells were also observed when pancreatic (PANC1 and Mia Paca2), colorectal (SW480 and HCT116), prostate (DU145 and PC3), and breast (MCF7 and MDA-MB-231) cancer cells were treated with 17AAG and the MEK1/2 inhibitor PD184352 (data not shown).

MEK1/2 Inhibitors and Geldanamycins Interact to Kill Hepatoma Cells via Activation of the Extrinsic Pathway

The molecular mechanisms by which MEK1/2 inhibitors and 17AAG interacted to kill hepatoma cells were next investigated in greater detail. Inhibition of caspase-9 function suppressed cell killing and abolished the greater than additive induction of cell killing by MEK1/2 inhibitors and 17AAG (Fig. 2A). Inhibition caspase-8 function (using the viral CRM A protein) blocked pro-caspase-9 and pro-caspase-3 cleavage and virtually abolished cell killing by MEK1/2 inhibitors and 17AAG (Fig. 2A; Supplementary Fig. S2).[6] We next used SV40 large T antigen transformed mouse embryonic fibroblasts that had been genetically modified to lack expression of proapoptotic proteins. MEK1/2 inhibitors and 17AAG enhanced cell killing in wild-type cells, whereas killing was significantly reduced

[6] Supplementary material for this article is available at Molecular Cancer Therapeutics Online (http://mct.aacrjournals.org/).

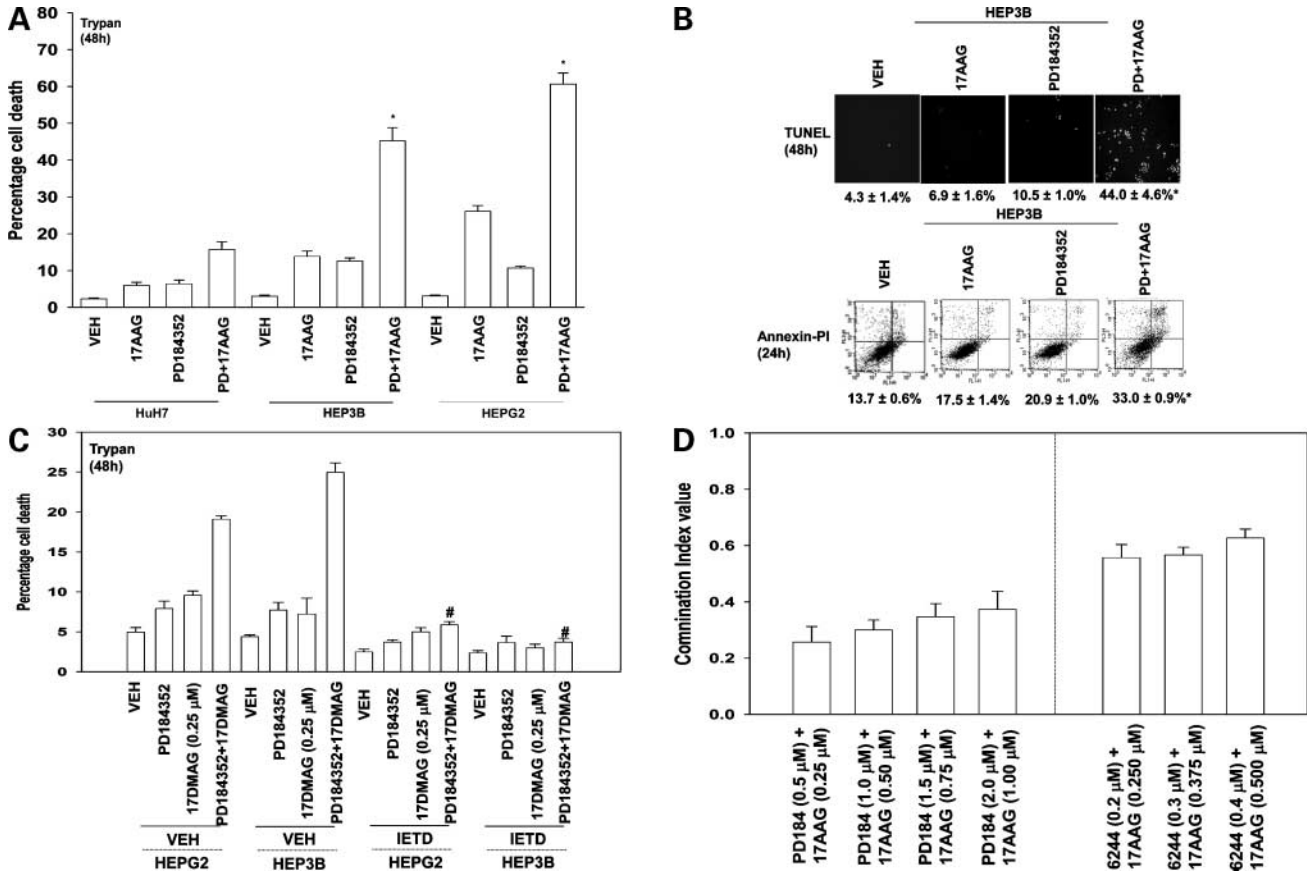

Figure 1. MEK1/2 inhibitors and 17AAG synergize to kill human hepatoma cells *in vitro*. **A,** human hepatoma cells (HuH7, HEPG2, and HEP3B) were treated 24 h after triplicate plating with vehicle (*VEH*), PD184352 (*PD*; 1 μmol/L), 17AAG (1 μmol/L), or both drugs combined. Cell viability was determined 48 h after drug treatment by trypan blue exclusion visible light microscopy assays in triplicate using a hemacytometer (± SE; $n = 3$ independent studies; *, $P < 0.05$, value greater amount of cell killing compared with vehicle-treated cells). **B,** human hepatoma cells (HEP3B) were treated 24 h after triplicate plating with vehicle, PD184352 (1 μmol/L), 17AAG (1 μmol/L), or both drugs combined. Cell viability was determined 24 or 48 h after drug treatment, as indicated, by Annexin V/propidium iodide flow cytometric assay and terminal deoxynucleotidyl transferase–mediated dUTP nick end labeling staining and fluorescent microscopy (± SE; $n = 3$ independent studies; *, $P < 0.05$, value greater amount of cell killing compared with vehicle-treated cells). **C,** human hepatoma cells (HEPG2 and HEP3B) were treated 24 h after triplicate plating with vehicle (DMSO) or the caspase-8 inhibitor IETD (50 μmol/L). Thirty minutes after caspase inhibitor treatment, cells were treated with vehicle, PD184352 (1 μmol/L), 17DMAG, or both drugs combined. Cell viability was determined 48 h after drug treatment as indicated by trypan blue exclusion visible light microscopy assays in triplicate using a hemacytometer (± SE; $n = 2$ independent studies; #, $P < 0.05$, value lower amount of cell killing compared with vehicle-treated cells). **D,** HEP3B cells were plated as single cells (250-1,500 per well) in sextuplicate and 12 h after plating treated with vehicle (DMSO), MEK1/2 inhibitors PD184352 (0.5-2.0 μmol/L) or AZD6244 (200-400 nmol/L), a geldanamycin (17AAG; 0.25-1.00 μmol/L), or both drugs combined as indicated at a fixed concentration ratio to perform median dose-effect analyses for synergy determination. After drug exposure (48 h), the medium was changed and cells were cultured in drug-free medium for 10 to 14 d. Cells were fixed and stained with crystal violet and colonies of >50 cells per colony were counted. Colony formation data were entered into the Calcusyn program and combination index values were determined. A combination index value of <1.00 indicates synergy. Mean ± SE combination index values from three separate studies.

in cells lacking expression of BAX, BAK, BIM, and BID (Fig. 2B). As inhibition of caspase-8 and loss of BID function negatively affected MEK1/2 inhibitor and 17AAG-induced killing, we did additional studies to define the relative role of caspase-8, and molecules upstream of caspase-8 that regulate its function, in the observed drug-induced cell killing process.

Overexpression of the caspase-8 inhibitor c-FLIP-s significantly reduced cell killing caused by MEK1/2 inhibitor and 17AAG treatment in hepatoma and pancreatic carcinoma cells (Fig. 3A and *B*). Overexpression of c-FLIP-s abolished the synergistic interaction between PD184352 (CI-1040) or AZD6244 (ARRY-142886) and 17AAG in true colony formation assays (Supplementary Table S1;[6] data not shown). Similar colony survival data were also obtained in PANC1 and Mia Paca2 cells (data not shown). In agreement with data in Fig. 2 showing that caspase-9 and BAX/BAK/BIM function also played a role in MEK1/2 inhibitor and 17AAG lethality, overexpression of the mitochondrial protective protein BCL-XL or the caspase-9 inhibitor XIAP suppressed cell killing. Treatment of HEP3B cells with MEK1/2 inhibitor and 17AAG caused cleavage of pro-caspase-8 and the proapoptotic protein BID and decreased expression of the caspase-8 inhibitor c-FLIP-s, effects that were prevented by constitutive overexpression of c-FLIP-s (Fig. 3B).

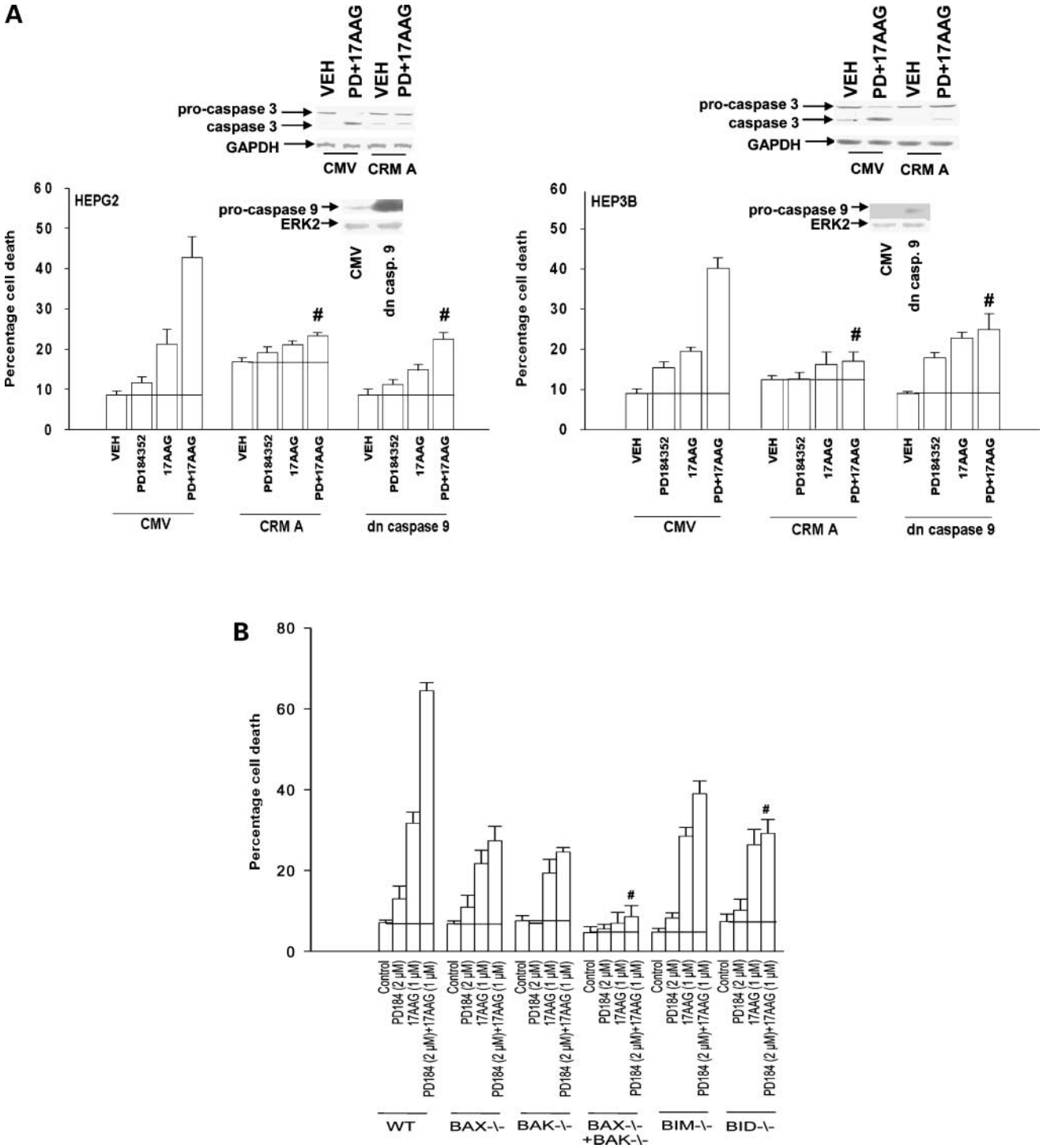

Figure 2. MEK1/2 inhibitors and 17AAG kill hepatoma cells via caspase-8- and caspase-9-dependent pathways. **A,** human hepatoma cells (HEPG2 and HEP3B) were infected 12 h after plating with either a control empty vector recombinant adenovirus [cytomegalovirus (CMV)], a recombinant virus to express CRM A, or a virus to express dominant-negative caspase-9. Twenty-four hours after virus infection, cells were treated with vehicle, PD184352, 17AAG, or both drugs combined. Cell viability was determined 48 h after drug treatment as indicated by trypan blue exclusion visible light microscopy assays in triplicate using a hemacytometer (± SE; $n = 2$ independent studies; #, $P < 0.05$, value lower amount of cell killing compared with vehicle-treated cells). *Topmost inset blotting,* cells were infected with CRM A and treated with drugs. Cells were isolated 48 h after exposure and SDS-PAGE and immunoblotting was done to determine the cleavage status of pro-caspase-3. **B,** SV40 large T antigen transformed mouse embryonic fibroblasts (wild-type) or deleted for both alleles of specific survival regulatory proteins 24 h after triplicate plating were treated with vehicle, PD184352, 17AAG, or both drugs combined. Cell viability was determined 48 h after drug treatment as indicated by trypan blue exclusion visible light microscopy assays in triplicate using a hemacytometer (± SE; $n = 2$ independent studies; #, $P < 0.05$ value lower amount of cell killing compared with vehicle-treated cells).

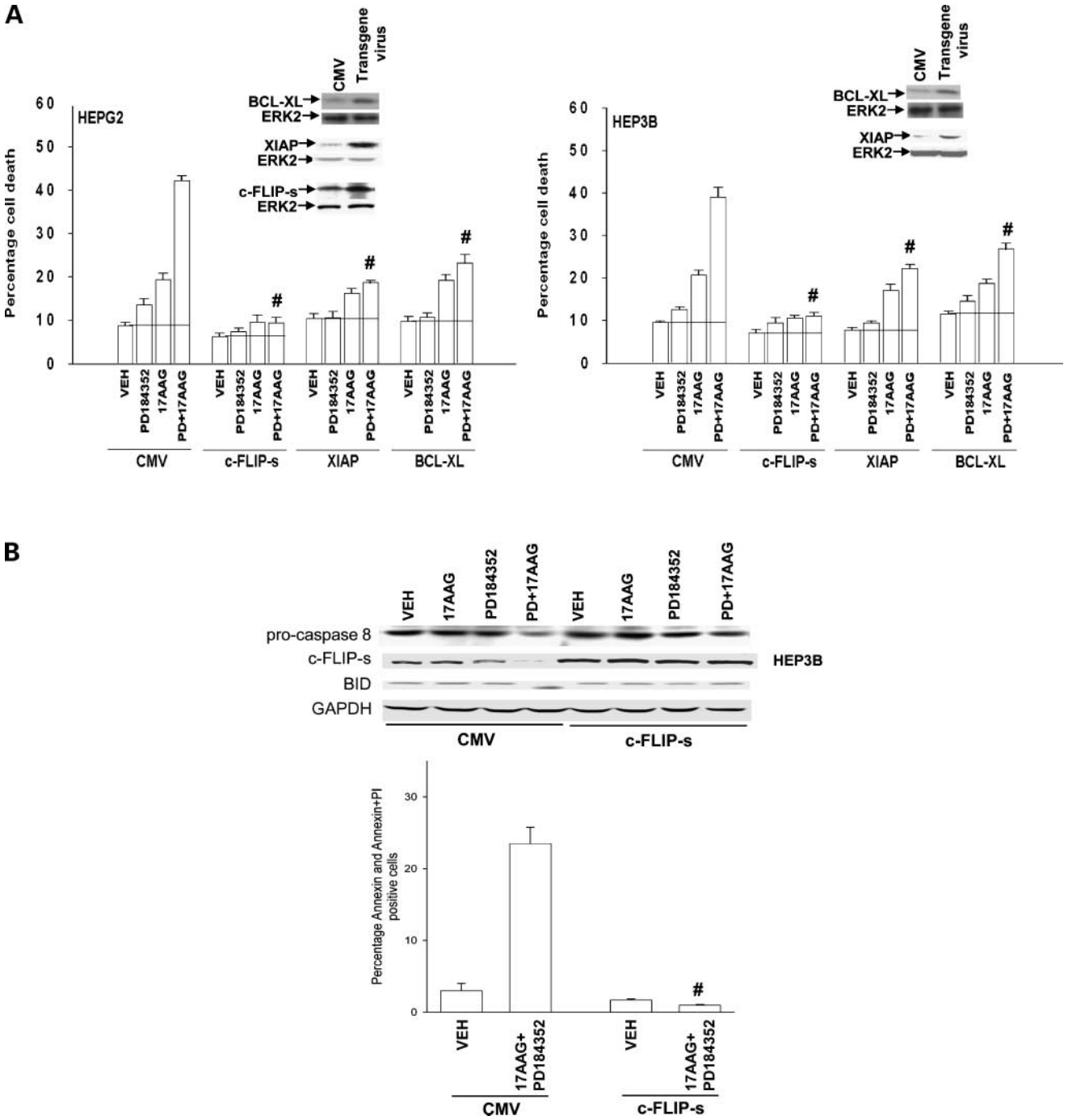

Figure 3. MEK1/2 inhibitors and 17AAG promote cell killing via a caspase-8-dependent pathway that requires suppression of c-FLIP-s expression. **A,** human hepatoma cells (HEPG2 and HEP3B) were infected 12 h after plating with either a control empty vector recombinant adenovirus (CMV), a recombinant virus to express c-FLIP-s, or a virus to express XIAP or BCL-XL. Twenty-four hours after virus infection, cells were treated with vehicle, PD184352, 17AAG, or both drugs combined. Cell viability was determined 48 h after drug treatment as indicated by trypan blue exclusion visible light microscopy assays in triplicate using a hemacytometer (± SE; $n = 2$ independent studies; #, $P < 0.05$, value lower amount of cell killing compared with vehicle-treated cells). **B,** *top immunoblotting section,* HEP3B cells were infected 12 h after plating with either a control empty vector recombinant adenovirus (CMV) or a recombinant virus to express c-FLIP-s. Twenty-four hours after virus infection, cells were treated with vehicle, PD184352, 17AAG, or both drugs combined. The expression/integrity of pro-caspase-8, BID, c-FLIP-s, and GAPDH was determined 24 h after drug treatment as indicated after SDS-PAGE and immunoblotting assays (representative of three studies). *Bottom graphical section,* human hepatoma cells (HEP3B) were infected 12 h after plating with either a control empty vector recombinant adenovirus (CMV) or a recombinant virus to express c-FLIP-s. Twenty-four hours after virus infection, cells were treated with vehicle, PD184352, 17AAG, or both drugs combined. Cell viability was determined 48 h after drug treatment as indicated by Annexin V/propidium iodide flow cytometric assay (± SE; $n = 2$ independent studies; #, $P < 0.05$, value lower amount of cell killing compared with vehicle-treated cells).

MEK1/2 Inhibitors and Geldanamycins Activate CD95 in Hepatoma Cells

Pro-caspase-8 is generally thought to be activated by binding to the FADD protein, which associates in a ''DISC'' with trimerized/activated death receptors such as TRAIL (DR4/DR5), tumor necrosis factor-α, or FAS (CD95; ref. 29). Previous studies by this laboratory in primary hepatocytes have strongly linked bile acid toxicity, and its promotion by inhibitors of MEK1/2, to ligand-independent activation and plasma membrane localization of CD95 (11, 30, 31).

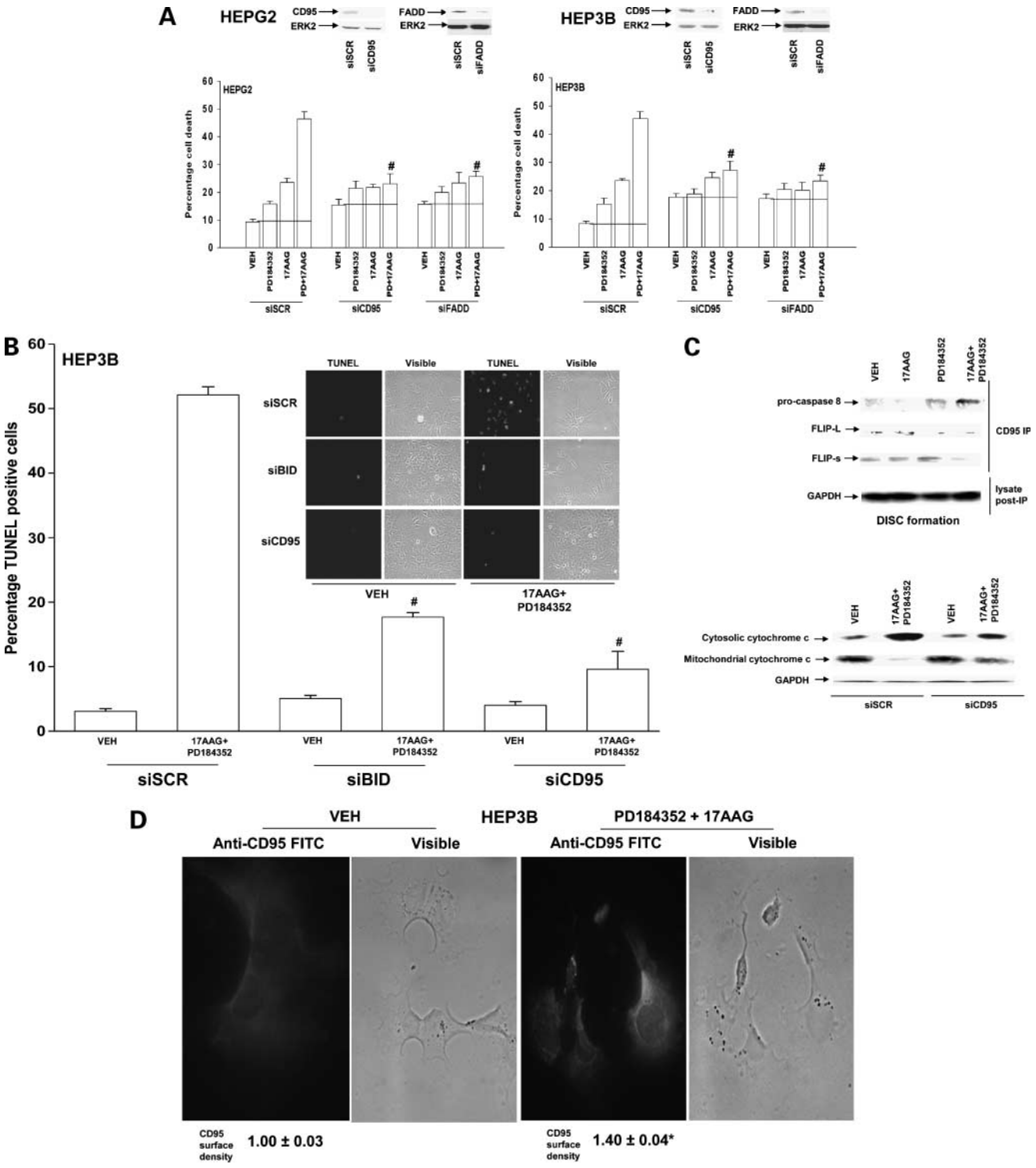

Knockdown of BID, FADD, or CD95 expression significantly reduced MEK1/2 inhibitor and 17AAG lethality in hepatoma cells (Fig. 4A and *B*; Supplementary Fig. S3).[6] Treatment of hepatoma cells with MEK1/2 inhibitor and 17AAG caused enhanced association of pro-caspase-8 with CD95 in immunoprecipitates of CD95 (DISC formation) and reduced the association of c-FLIP-s with CD95 (Fig. 4C, *top*). Treatment of hepatoma cells with MEK1/2 inhibitor and 17AAG caused release of cytochrome *c* into the cytosol from the mitochondria and decreased mitochondrial levels of cytochrome *c*, an effect that was suppressed by knockdown of CD95 expression (Fig. 4C, *bottom*).

Based on prior studies in primary hepatocytes with bile acids and CD95 activation, we determined whether treatment of hepatoma cells with MEK1/2 inhibitor and 17AAG elevated the plasma membrane levels/surface density of CD95 indicative of CD95 activation. Treatment of hepatoma cells with PD184352 and 17AAG visibly increased plasma membrane staining for CD95 in HEP3B and HEPG2 cells, an effect that we were also able to quantitate (Fig. 4D; data not shown). Collectively, these findings show that treatment of hepatoma cells with MEK1/2 inhibitors and 17AAG promotes CD95 activation, DISC formation with caspase-8 association, and extrinsic pathway activation, which leads to BID cleavage, mitochondrial dysfunction, and cell death.

MEK1/2 Inhibitors and Geldanamycins Interact to Reduce AKT and ERK1/2 Activities *In vitro* That Are Essential to Maintain Antiapoptotic Protein Expression

Further studies then attempted to define the changes in signal transduction pathway function, which were causal in the regulation of the extrinsic pathway in cells treated with MEK1/2 inhibitors and 17AAG. Combined exposure of hepatoma cells to MEK1/2 inhibitor and 17AAG resulted in a rapid phosphorylation of p38 MAPK within 3 h and lasting for ~24 h, a rapid dephosphorylation of ERK1/2 over 3 to 24 h, and a slower modest secondary decline in AKT (S473) phosphorylation that occurred over 6 to 24 h (Fig. 5A). Of note, at the concentration of PD184352 used (1 μmol/L) in our studies, ERK1/2 phosphorylation was not completely suppressed over 24 h. The JNK1/2 pathway was not activated under our culture/treatment conditions (data not shown). The changes in signaling pathway activity approximately correlated with the prolonged reduced expression of c-FLIP-s, BCL-XL, and XIAP, which was in general agreement with our prior data showing that overexpression of c-FLIP-s, BCL-XL, and XIAP protected hepatoma cells from MEK1/2 inhibitor and 17AAG treatment.

We next determined whether constitutive activation of MEK1 and/or AKT could suppress the toxic interaction between 17AAG and the MEK1/2 inhibitor PD98059. PD98059 was chosen for these studies because, unlike PD184352 and AZD6244, it is a relatively poor inhibitor of the constitutively activated MEK1 EE protein. Combined expression of activated MEK1 and activated AKT, but not either protein individually, maintained ERK1/2 and AKT (S473) phosphorylation in the presence of the MEK1/2 inhibitor PD98059 and 17AAG and suppressed drug-induced phosphorylation of p38 MAPK (Supplementary Fig. S4).[6] In HEPG2 cells, expression of constitutively active AKT more strongly suppressed the lethality of 17AAG and MEK1/2 inhibitor treatment than expression of constitutively active MEK1, whereas, in HEP3B cells, both constitutively active AKT and constitutively active MEK1 were apparently equally competent at blunting drug toxicity (Fig. 5B; Supplementary Fig. S5).[6] In both hepatoma cell types, combined expression of constitutively active AKT and constitutively active MEK1 almost abolished 17AAG- and PD98059-induced cell killing. Expression of constitutively active AKT and constitutively active MEK1 maintained the expression levels of c-FLIP-s and well as those of XIAP and BCL-XL in cells treated with 17AAG and PD98059 (Fig. 5B, *top inset immunoblotting*).

Figure 4. MEK1/2 inhibitors and 17AAG kill hepatoma cells in a CD95-FADD-caspase-8-BID-dependent manner. **A** and **B,** HEPG2 and HEP3B cells were transfected with either a scrambled siRNA molecule (*siSCR*) or validated siRNA molecules to knockdown the expression of CD95, FADD, BID, or c-FLIP-s. Twelve hours after transfection, cells were replated. Twenty-four hours after replating, cells were treated with vehicle, PD184352, 17AAG, or both drugs combined. Cell viability was determined 48 h after drug treatment as indicated by terminal deoxynucleotidyl transferase–mediated dUTP nick end labeling assay and fluorescent light microscopy or by trypan blue exclusion visible light microscopy assays in triplicate using a hemacytometer as indicated (± SE; $n = 2$ independent studies for each method; #, $P < 0.05$, value lower amount of cell killing compared with vehicle-treated cells). **A,** *inset immunoblotting sections,* 36 h after siRNA transfection to knockdown the expression of CD95 and FADD, cells were isolated and subjected to immunoblotting to determine the expression of CD95 and FADD and GAPDH loading control ($n = 2$). Data for knockdown of c-FLIP-s and BID are not shown. **C,** *top,* HEP3B cells 24 h after plating were treated with vehicle, PD184352, 17AAG, or both drugs combined. Six hours after drug exposure, cells were lysed and CD95 was immunoprecipitated as described in Materials and Methods based on established protocols. SDS-PAGE and immunoblotting was done to determine the levels of pro-caspase-8 and c-FLIP isoforms in the immunoprecipitates and the level of GAPDH in the cell lysates following immunoprecipitation. *Bottom,* HEP3B cells were transfected with either a scrambled siRNA molecule or a validated siRNA molecule to knockdown the expression of CD95. Twelve hours after transfection, cells were replated. Twenty-four hours after replating, cells were treated with vehicle, PD184352, 17AAG, or both drugs combined. Twelve hours after drug treatment, cells were isolated and the cytosolic and membrane/mitochondrial fractions of the cells were purified as described in Materials and Methods. The amount of cytosolic and mitochondrial-associated cytochrome *c* was determined by SDS-PAGE followed by immunoblotting ($n = 3$). **D,** HEP3B cells 24 h after plating into four-well glass slides were treated with vehicle, PD184352, 17AAG, or both drugs combined. Six hours after drug exposure, cells were fixed *in situ*, but were not permeabilized, and stained with a FITC-labeled anti-CD95 antibody. Studies with a nonspecific identical subtype antibody as a control showed the observed effects were CD95 dependent. Identical analyses were also done on any new batch of antibody used over the course of the studies. Cells were visualized under fluorescent light. Representative field from four separate/independent experiments. To mathematically prove that our visual observation was actually significant, the mean increase in CD95 surface fluorescence was determined by analyzing 5 cells from vehicle or 17AAG + PD184352 conditions with 20 individual random areas of fluorescent density determination per cell (100 density determinations in total ± SE) with at least one cell per experiment, and this value is presented below the pictorial data in the figure. *, $P < 0.05$, value greater amount of cell surface CD95 compared with vehicle-treated cells.

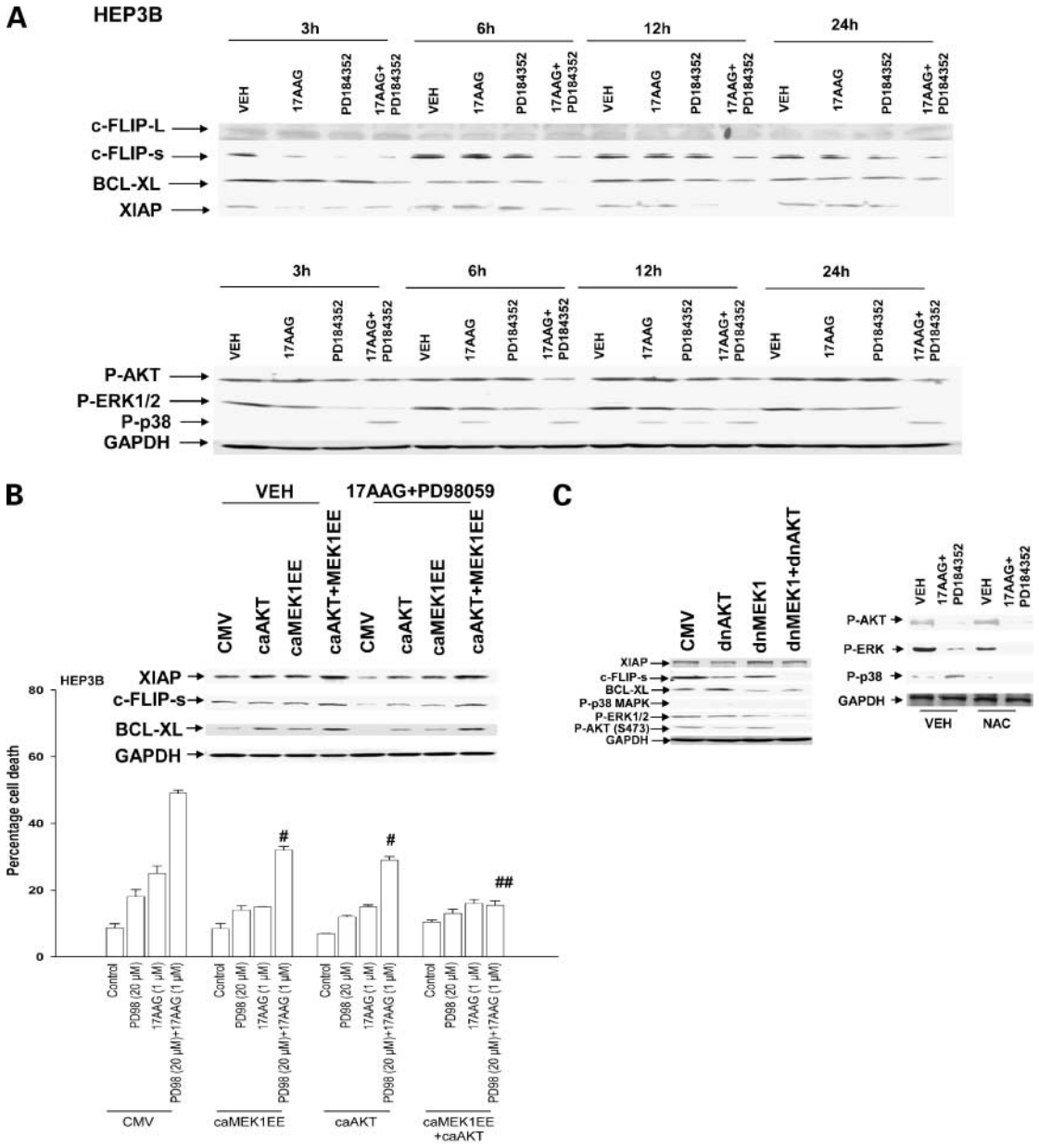

Figure 5. Combined exposure to MEK1/2 inhibitor and 17AAG results in prolonged suppression of ERK1/2 and AKT phosphorylation and prolonged suppression of c-FLIP-s, BCL-XL, and XIAP levels. **A,** HEP3B cells 24 h after plating were treated with vehicle, PD184352, 17AAG, or both drugs combined. At the indicated times after drug exposure, cells were isolated and subjected to SDS-PAGE followed by immunoblotting to determine the phosphorylation of ERK1/2, AKT (S473), and p38 MAPK and the expression of FLIP-l, FLIP-s, BCL-XL, XIAP, and GAPDH (n = 3-4). **B,** HEPG2 and HEP3B cells 12 h after plating in triplicate were infected with either a control empty vector recombinant adenovirus (CMV), a recombinant virus to express constitutively active MEK1 EE, a recombinant virus to express constitutively active AKT, or both viruses to express activated AKT and MEK1 EE. Twenty-four hours after infection, as indicated, cells were treated with either vehicle, PD98059, or both drugs combined. *Bottom graphical sections,* HEPG2 and HEP3B cells were isolated 48 h after drug exposure and cell viability was determined as indicated by trypan blue exclusion visible light microscopy assays in triplicate using a hemacytometer (± SE; n = 3). #, $P < 0.05$, value less lethality compared with corresponding value in CMV-infected cells; ##, $P < 0.05$, value less lethality compared with corresponding value in constitutively activated AKT-infected and constitutively activated MEK1-infected cells. *Inset,* HEP3B cells expressing activated AKT and MEK1 EE and treated with PD98059 and 17AAG, or their appropriate parallel control cells, were isolated 24 h after drug exposure and following SDS-PAGE immunoblotting done to determine the expression of c-FLIP-s, BCL-XL, and XIAP (n = 2 independent studies). **C,** *blotting to left,* HEP3B cells expressing either a control empty vector recombinant adenovirus (CMV), a recombinant virus to express dominant-negative MEK1, a recombinant virus to express dominant-negative AKT, or both viruses to express dominant-negative AKT and dominant-negative MEK1 were isolated 48 h after infection and processed for SDS-PAGE to determine the expression of c-FLIP-s, BCL-XL, and XIAP and the phosphorylation of ERK1/2, AKT (S473), and p38 MAPK (n = 2 independent studies). *Blotting to right,* HEP3B cells were treated with either vehicle (PBS) or with *N*-acetylcysteine (20 mmol/L) 30 min before treatment with vehicle (DMSO) or with MEK1/2 inhibitor PD184352 (1 μmol/L) and geldanamycin (17AAG, 1 μmol/L). Cells were isolated 24 h after drug exposure and the phosphorylation of ERK1/2, AKT (S473), and p38 MAPK was determined after SDS-PAGE by immunoblotting (n = 2 independent studies).

MEK1/2 Inhibitors and Geldanamycins Interact to Promote p38 MAPK Activation That Is in Part Reactive Oxygen Species Dependent and Suppressed by AKT and ERK1/2 Signaling: CD95 Activation after Drug Exposure Is p38 MAPK Dependent

As noted in Fig. 5A, the p38 MAPK pathway was rapidly activated within 3 h after combined exposure to 17AAG and MEK1/2 inhibitor before complete inactivation of ERK1/2 and AKT that occurred 6 to 12 h after exposure, suggesting that although activated MEK1 and activated AKT can suppress drug-induced p38 MAPK activation the activation of p38 MAPK was likely to be independent of drug-induced ERK1/2 and AKT inactivation (Fig. 5A; Supplementary Fig. S4).[6] Combined expression of dominant-negative MEK1 and dominant-negative AKT reduced the phosphorylation of ERK1/2 and AKT but did not profoundly increase the phosphorylation of p38 MAPK (Fig. 5C, *blots to the left*). Combined expression of dominant-negative MEK1 and dominant-negative AKT reduced the expression of c-FLIP-s and BCL-XL but did not significantly enhance basal levels of cell morbidity (Fig. 5B; data not shown). Expression of dominant-negative MEK1 recapitulated the effects of PD184352 in terms of enhancing 17AAG-stimulated p38 MAPK phosphorylation and enhancing 17AAG-stimulated killing (data not shown). These findings argue that the drug 17AAG must provide an additional ''signal'' separate from simply suppressing ERK1/2 and AKT function, which is required to cause p38 MAPK activation and to promote tumor cell killing.

Prior studies from this laboratory have shown that reactive oxygen species (ROS) are an important component of 17AAG lethal signaling, including the activation of p38 MAPK (3, 27). Exposure of hepatoma cells to the ROS quenching agent *N*-acetylcysteine, which suppresses ROS induction in hepatoma cells, did not significantly modify the inactivation of ERK1/2 or AKT by 17AAG and MEK1/2 inhibitor treatment but did suppress the activation of p38 MAPK by these drugs (Fig. 5C, *blots to the right*; data not shown; ref. 27). Exposure of hepatoma cells to the ROS quenching agent *N*-acetylcysteine significantly reduced the lethality of 17AAG and MEK1/2 inhibitor treatment (data not shown). Collectively, the data in Fig. 5 argue that loss of ERK1/2 and AKT function and gain of p38 MAPK function play important roles in the lethal actions of 17AAG and MEK1/2 inhibitor treatment in hepatoma cells.

Based on our data in Fig. 5A, which showed that p38 MAPK was rapidly activated after combined exposure to 17AAG and MEK1/2 inhibitor, we further investigated whether this signaling pathway played any direct role in the regulation of CD95 and the extrinsic pathway following drug treatment. Exposure of cells to 17AAG and PD184352 increased the association of pro-caspase-8 with CD95 in hepatoma cells (DISC complex formation), an effect that was inhibited by expression of dominant-negative p38 MAPK or by expression of dominant-negative MKK3 and dominant-negative MKK6 [Fig. 6A, *section* (*i*)]. Expression of dominant-negative p38 was competent to inhibit stress-induced signaling in this pathway (data not shown). Expression of activated AKT and activated MEK1 also suppressed 17AAG and MEK1/2 inhibitor-induced association of pro-caspase-8 with CD95 [Fig. 6A, *section* (*ii*)]. Expression of neither dominant-negative p38 MAPK nor activated AKT and activated MEK1 altered the whole-cell expression levels of either CD95 or FAS ligand (Supplementary Fig. S6).[6] This suggests that CD95 activation was p38 MAPK dependent and FAS ligand independent.

Expression of dominant-negative p38 visibly suppressed the drug-induced plasma membrane staining for CD95, which was quantified (Fig. 6B). Expression of dominant-negative p38 MAPK, but not inhibition of the JNK1/2 pathway, suppressed 17AAG and MEK1/2 inhibitor-induced cell killing in HEPG2 and HEP3B cells (Fig. 6C; Supplementary Fig. S7;[6] data not shown). The data in Fig. 6A argued that inhibition of p38 MAPK prevented the association of pro-caspase-8 and CD95. MEK1/2 inhibitor and 17AAG-induced activation of BAX and BAK, proteins that act downstream of CD95 to cause mitochondrial dysfunction, was also shown to be p38 MAPK dependent (Fig. 6C, *top inset*). Thus, 17AAG and MEK1/2 inhibitors, from a signal transduction standpoint, interact to kill human hepatoma cells *in vitro* by suppressing AKT and ERK1/2 activity and by activating p38 MAPK, and these pathways regulate cell survival both at the level of CD95 and at the level of the mitochondrion within the tumor cell.

MEK1/2 Inhibitors and Geldanamycins Interact to Kill Hepatoma Cells in a Synergistic Fashion *In vivo*

Finally, as both 17AAG and MEK1/2 inhibitors are under evaluation in the clinic, we tested whether our *in vitro* findings could be translated into animal model systems. We noted that unselected clones of HEP3B and HEPG2 cells are poorly tumorigenic in the flanks of athymic mice and form tumors that rapidly become necrotic on growth beyond >200 mm^3 potentially due to a relatively low CD31 staining (data not shown). As such, we chose an *in vivo* treatment, *ex vivo* colony formation assay approach to assess tumor cell killing and long-term survival as well as immunohistochemical variables. HEP3B tumors exposed to PD184352 and 17AAG *in vivo* had a lower *ex vivo* cell colony-forming ability than tumor cells exposed to either agent individually that correlated with increased caspase-3 cleavage and reduced phosphorylation of ERK1/2 and AKT in the tumor and increased p38 MAPK phosphorylation (Fig. 6D). The expression of c-FLIP-s was also reduced in HEP3B tumors exposed to 17AAG and PD184352 that were undergoing apoptosis, arguing that this protein is both mechanistically linked to modulation of the killing process *in vitro* and *in vivo* and that c-FLIP-s expression could be used as a surrogate marker for tumor responsiveness to this drug combination *in vivo*.

Discussion

Prior *in vitro* studies from our laboratories in chronic myelogenous leukemia cells have noted that inhibitors of MEK1/2 enhanced geldanamycin lethality by promoting

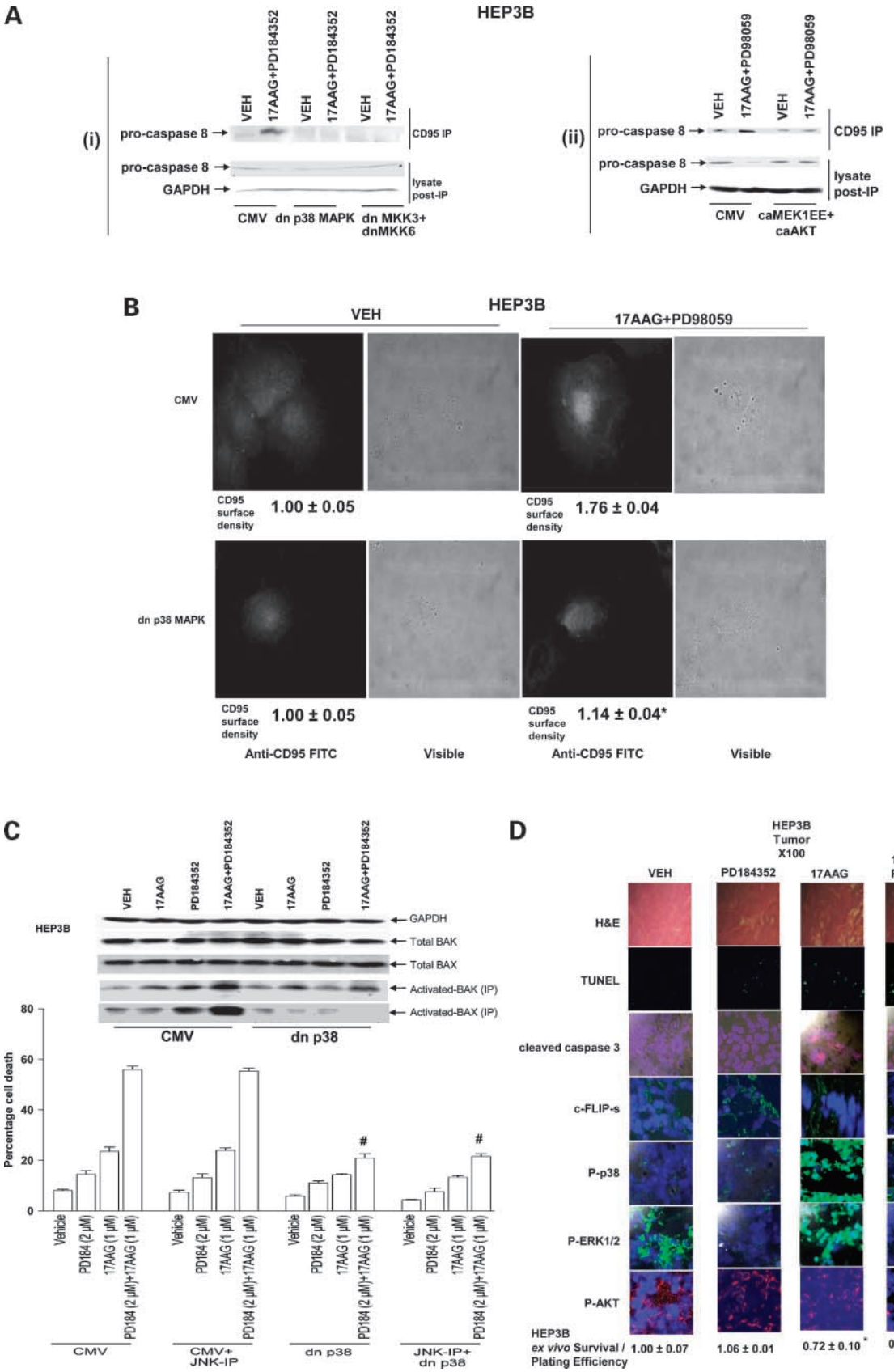

mitochondrial dysfunction (28). The present studies focused more precisely on defining the mechanism(s) by which these agents altered cell survival in hepatoma and pancreatic cancer cells *in vitro*.

Our findings showed that combined exposure of tumor cells to 17AAG and MEK1/2 inhibitors (PD98059; PD184352; AZD6244) promoted inhibition of the ERK1/2 and AKT pathways and activation of the p38 MAPK pathway. The reduced activity within the ERK1/2 and AKT pathways lowered the cell death threshold of hepatoma cells at multiple points within the extrinsic and intrinsic apoptosis pathways as judged by suppressed protein levels of c-FLIP-s, BCL-XL, and XIAP, whose reduced levels of expression could be rescued by molecular activation of AKT and MEK1. Drug-induced activation within the p38 MAPK pathway was a proapoptotic stimulus as judged by p38 MAPK dependent: CD95 localization in the plasma membrane, CD95 association with pro-caspase-8, and activation of BAX and BAK. Loss of MEK1/2 and AKT pathway function reduced c-FLIP-s expression and in parallel facilitated activation of p38 MAPK. Without suppression of c-FLIP-s levels activation of CD95 was incapable of promoting caspase-8 activation/tumor cell killing regardless of downstream BAX and BAK activation and inhibition of BCL-XL and XIAP expression. This argues that modulation of c-FLIP-s levels represented a key nodal point proximal to CD95 death receptor activation for the manifestation of 17AAG and MEK1/2 inhibitor toxicity in tumor cells (Supplementary Fig. S8).[6]

HSP90 antagonists, of which the ansamycin analogue geldanamycin and its less toxic derivatives, 17AAG and 17DMAG, represent the prototypes, have become a focus of considerable interest as antineoplastic agents, and clinical trials involving 17AAG and 17DMAG have been initiated over the last 5 to 10 years (e.g., ref. 21). These agents act by disrupting the chaperone function of HSP90, leading to the ultimate proteasomal degradation of diverse signal transduction regulatory proteins implicated in the neoplastic cell survival, including Raf-1, B-Raf, AKT, and ERBB family receptors. Mutant active kinase proteins, including activated B-Raf and Bcr-Abl, have been noted to be particularly susceptible to agents that disrupt HSP90 function (e.g. ref. 20). The basis for the tumor cell selectivity of 17AAG is not definitively known; however, there is evidence that HSP90 derived from tumor cells has an increased affinity for geldanamycins compared with HSP90 protein obtained from normal cells (32). One difficulty with the development of 17AAG has been the limited water solubility of this drug and an analogue of 17AAG, 17DMAG, which is considerably more water-soluble than 17AAG, has been synthesized. MEK1/2 inhibitors were shown previously to enhance the lethality of 17DMAG in chronic myelogenous leukemia cells and evidence from our present analyses indicates that

Figure 6. CD95 activation by MEK1/2 inhibitors and 17AAG is p38 MAPK dependent. **A,** *section* (*i*), HEP3B cells 12 h after plating were infected with either a control empty vector recombinant adenovirus (CMV), a recombinant virus to express dominant-negative p38α MAPK, or viruses to express dominant-negative forms of MKK3 and MKK6. Twenty-four hours after infection, as indicated, cells were treated with either vehicle, PD184352, or PD98059 as indicated, 17AAG, or the drugs in combination. Six hours after drug exposure, cells were lysed and CD95 was immunoprecipitated as described in Materials and Methods. SDS-PAGE and immunoblotting were done to determine the levels of pro-caspase-8 in the immunoprecipitates and the level of pro-caspase-8 and GAPDH in the cell lysates following immunoprecipitation ($n = 3$ independent studies). *Section* (*ii*), HEP3B cells 12 h after plating were infected with either a control empty vector recombinant adenovirus (CMV) or recombinant adenoviruses to express constitutively active forms of MKK1 EE and AKT. Twenty-four hours after infection, as indicated, cells were treated with either vehicle (DMSO) or the combination of PD184352 and 17AAG. Six hours after drug exposure, cells were lysed and CD95 was immunoprecipitated as described in Materials and Methods. SDS-PAGE and immunoblotting was done to determine the levels of pro-caspase-8 in the immunoprecipitates and the level of pro-caspase-8 and GAPDH in the cell lysates following immunoprecipitation ($n = 2$ independent studies). **B,** HEP3B cells 12 h after plating into four-chamber glass slides were infected with either a control empty vector recombinant adenovirus (CMV) or a recombinant virus to express dominant-negative p38α MAPK. Twenty-four hours after infection, as indicated, cells were treated with either vehicle or the combination of PD98059 and 17AAG. Six hours after drug exposure, cells were fixed *in situ*, but were not permeabilized, and stained with a FITC-labeled anti-CD95 antibody. Studies with a nonspecific identical subtype antibody as a control showed that the observed effects were CD95 dependent. Identical analyses were also done on any new batch of antibody used over the course of the studies. Cells were visualized under fluorescent light. Representative field from four separate/independent experiments. To mathematically prove that our visual observation was actually significant, the mean increase in CD95 surface fluorescence was determined by analyzing 5 cells from vehicle or 17AAG + PD184352 conditions with 20 individual random areas of fluorescent density determination per cell (100 density determinations in total ± SE) with at least one cell per experiment, and this value is presented below the pictorial data in the figure. *, $P < 0.05$, value greater amount of cell surface CD95 compared with vehicle-treated cells. **C,** HEP3B cells 12 h after plating were infected with either a control empty vector recombinant adenovirus (CMV) or a recombinant virus to express dominant-negative p38α MAPK. Twenty-four hours after infection, as indicated, cells were pretreated with vehicle (DMSO) or a JNK inhibitory peptide (*JNK-IP*; 10 μmol/L) followed 30 min later by treatment with either vehicle, PD184352, 17AAG, or both drugs combined. Cells were isolated 48 h after drug exposure and cell viability was determined as indicated by trypan blue exclusion visible light microscopy assays in triplicate using a hemacytometer (± SE; $n = 3$ independent studies). #, $P < 0.05$, value less than amount of killing compared with CMV-infected cells. *Top inset,* HEP3B cells 12 h after plating were infected with either a control empty vector recombinant adenovirus (CMV) or a recombinant virus to express dominant-negative p38α MAPK. Twenty-four hours after infection, as indicated, cells were treated with either vehicle, PD184352, 17AAG, or both drugs combined. Cells were isolated 6 h after drug exposure and immunoprecipitations were done to isolate activated forms of BAX and of BAK from each treatment condition. SDS-PAGE was done on immunoprecipitates and on total cell lysates to determine the total and activated levels of BAX and BAK in treated cells ($n = 2$ independent studies). **D,** HEP3B cells (10^7) were injected into the rear right flanks of athymic mice and tumors were permitted to form (~150 mm^3). Animals were treated with 17AAG and MEK1/2 inhibitor PD184352 as described in Materials and Methods for 30 h after which tumors were isolated, sectioned, portions macerated, and digested to obtain individual tumor cells for *ex vivo* colony formation assays. *Bottom numerical section,* true percentage plating efficiency of tumor cells in *ex vivo* colony formation assays from two tumors plated each in sextuplicate at multiple cell dilutions (2,000-4,000 cells per well) ± SE. In parallel, on sectioned portions of the isolated tumors, staining was done to determine H&E (morphology) and terminal deoxynucleotidyl transferase–mediated dUTP nick end labeling (apoptosis) as well as immunohistochemistry with 4′,6-diamidino-2-phenylindole counterstaining (*dark blue/mauve nuclei*); the cleavage status of caspase-3 (*cherry red*); the expression of c-FLIP-s (*green*); and the phosphorylation status of ERK1/2 (*green*), p38 MAPK (*green*), and AKT (S473; *cherry red*). Representative of two independent experiments.

PD184352 also enhances 17DMAG lethality in human hepatoma cells (28).

Although some hepatoma tumors have been noted to express mutated active forms of Ras and B-Raf proteins, the penetrance of such mutations within the hepatoma patient population as a whole has not been noted to be as prevalent as the well-described high mutational rate of these proteins found in other gastrointestinal malignancies such as pancreatic adenocarcinoma or colorectal carcinoma (33, 34). Of note, however, is that 17AAG and MEK1/2 inhibitors interact to kill pancreatic carcinoma cells. Mutations in phosphatidylinositol 3-kinase and loss of PTEN function/expression in hepatoma have also been noted (35, 36). These findings would suggest that the lethal interaction of 17AAG with MEK1/2 inhibitors we observed in HuH7, HEPG2, and HEP3B hepatoma cells or in other unrelated epithelial tumor cell types is unlikely to be due to a simple suppression of a small subset of hyperactivated HSP90 client proteins as would be predicted based on expression of, for example, mutated active B-Raf or K-Ras. In contrast to pancreatic or colorectal malignancies, virally induced cancers (e.g., by hepatitis B virus; the HEP3B cell line is an example), are more prevalent in liver cancers and the key transforming protein of hepatitis B virus, pX, has been shown by many groups, including this laboratory, to increase the activities of the ERK1/2, AKT, and JNK1/2 pathways and enhance the expression of cell cycle regulatory proteins such as p16, p21, and p27 in primary hepatocytes in a dose-dependent manner (37–39). At present, there are no published studies indicating whether pX is a HSP90 client protein. Based on the concept of oncogene addiction, however, hepatoma cells such as HEP3B-expressing pX could in theory have higher basal levels of ERK1/2 and AKT activity, which would in turn make them more susceptible to cell death processes following inhibition of these signal transduction pathways by 17AAG and MEK1/2 inhibitor exposure. Further studies will be required to determine definitively whether hepatitis B virus–infected hepatoma isolates are more sensitive to the 17AAG and MEK1/2 inhibitor drug combination than those lacking transforming hepatitis B virus proteins.

The Raf-MEK1/2-ERK1/2 pathway exerts cytoprotective actions in a wide variety of transformed cell types, which has lead to the development of multiple pharmacologic inhibitors of the pathway, including inhibitors of Ras farnesylation and geranylgeranylation, the multikinase and Raf inhibitor sorafenib, and the MEK1/2 inhibitors PD184352, PD0325901, and AZD6244 (40–42). PD184352 has undergone clinical evaluation in phase I and II trials involving patients with advanced malignancies and inhibition of ERK1/2 phosphorylation in tumor tissues and peripheral blood mononuclear cells was observed at higher drug doses, indicating that achieving desired pharmacodynamic effects *in vivo* was feasible. However, the relative pharmacodynamic profile of PD184352 was not considered to be optimal, and as a single agent, the drug did not generate any objective tumor growth delay responses in a phase II trial (43). More potent MEK1/2 inhibitors with superior pharmacokinetic characteristics (PD0325901; AZD6244) are currently undergoing clinical evaluation; encouragingly, our present studies showed that AZD6244 and 17AAG were competent to interact in a synergistic fashion to kill tumor cells via an extrinsic pathway-dependent mechanism. Studies beyond the scope of the present article will be required to determine whether PD0325901 and AZD6244 can interact with 17DMAG *in vitro* and *in vivo* to kill human hepatoma and other carcinoma cell types.

We noted that administration of low concentrations of PD184352 or of 17AAG in hepatoma cells resulted in an initial abrogation of ERK1/2 phosphorylation followed by a gradual recovery toward vehicle control-treated levels. On the other hand, coadministration of PD184352 and 17AAG resulted in the profound and sustained dephosphorylation of ERK1/2 throughout the entire measured 24 h exposure interval. Similarly, only under conditions of drug coadministration was a more modest AKT (S473) dephosphorylation observed. In view of evidence that the duration of MEK/ERK and AKT signaling plays a critical role in the biological consequences of activation of these pathways, it is tempting to speculate that sustained inactivation of both ERK1/2 and AKT signaling partially contributes to the lethality of the PD184352 and 17AAG drug regimen in these cells.

The relative roles of ERK1/2 versus AKT inactivation in the promotion of cell killing by 17AAG and MEK1/2 inhibitor treatment were also noted to be slightly different comparing HEPG2 and HEP3B cells. In HEPG2 cells, expression of constitutively active MEK1 did not significantly protect cells from 17AAG and MEK1/2 inhibitor toxicity, whereas expression of activated AKT reduced toxicity by ~50%. In HEPG2 cells, expression of activated MEK1 in the presence of activated AKT, however, abolished 17AAG and MEK1/2 inhibitor toxicity. In HEP3B cells, both activated MEK1 and activated AKT each approximately equally contributed to suppressing cell killing induced by17AAG and MEK1/2 inhibitor exposure. There are many examples of this form of cell behavior where in some cell types survival is mediated primarily by the actions of one pathway with a secondary or nonexistent protective role for other pathways and in others where survival is shared between many pathways. In hepatocytes/hepatoma cells, the regulation of c-FLIP protein expression has been linked to both ERK1/2 and AKT pathways (e.g., refs. 11, 44). Thus, in the majority of malignancies, based on tumor cell heterogeneity within the tumor, the likelihood that specific inhibition of only one signaling module will achieve a measurable prolonged therapeutic effect will probably be small, which may explain why, even when ERK1/2 phosphorylation was significantly suppressed in patient tumors in the presence of PD184352, little benefit was clinically observed. As 17AAG not only will inhibit the ERK1/2 and AKT pathways, and in the presence of a MEK1/2 inhibitor act to cause prolonged suppression of pathway function, but also will furthermore reduce the stability of additional cytoprotective HSP90 client proteins such as hypoxia-inducible factor-1α, our data

argue that the simultaneous targeting of multiple protective pathways by 17AAG and MEK1/2 inhibitors may represent a ubiquitous and better approach to kill cancer cells (45). In a similar vein to reliance on one pathway for a major cellular effect, resistance to 17AAG and MEK1/2 inhibitor exposure could in theory be mediated by reduced expression levels of the death receptor CD95; indeed, HuH7 cells, which have very low expression of CD95, were relatively resistant to drug exposure killing compared with HEPG2 and HEP3B cells (46).

Geldanamycins are known to have the capacity to generate ROS in gastrointestinal tumor cells (47); prior studies from our laboratory have also shown 17AAG to induce ROS in primary hepatocytes and hepatoma cells (3, 27, 48). Our data argued that ROS production was a key component in p38 MAPK activation after 17AAG and MEK1/2 inhibitor exposure together with suppression of ERK1/2 and AKT activity. As AZD6244 has recently been shown to reduce hepatoma growth *in vivo*, collectively, with our present findings, including our *in vivo* data using HEP3B, and in Mia Paca2 cells,[7] it is tempting to speculate that the 17AAG and MEK1/2 inhibitors could have *in vivo* potential as a therapeutic tool in the treatment of hepatoma and pancreatic cancer (49). Additional studies of will be required to determine whether and how 17AAG and/or 17DMAG and MEK1/2 inhibitors interact *in vivo* to suppress tumor cell viability and growth.

Disclosure of Potential Conflicts of Interest

No potential conflicts of interest were disclosed.

Acknowledgments

P. Dent thanks Dr. Shigang Lin for performing some of the initial work on these studies.

[7] M.A. Park, H. Hamed, and P. Dent, unpublished findings.

References

1. Akriviadis EA, Llovet JM, Efremidis SC, et al. Hepatocellular carcinoma. Br J Surg 1998;85:1319 – 31.

2. Parkin DM, Bray F, Ferlay J, Pisani P. Global cancer statistics, 2002. CA Cancer J Clin 2005;55:74 – 108.

3. Dent P. MAP kinase pathways in the control of hepatocyte growth, metabolism and survival. In: Dufour JF, Clavien P-A, editors. Signaling pathways in liver diseases. Springer Press; 2005. Chapter 19. p. 223 – 38.

4. Dent P, Yacoub A, Fisher PB, Hagan MP, Grant S. MAPK pathways in radiation responses. Oncogene 2003;22:5885 – 96.

5. Valerie K, Yacoub A, Hagan MP, et al. Radiation-induced cell signaling: inside-out and outside-in. Mol Cancer Ther 2007;6:789 – 801.

6. Hawkins W, Mitchell C, McKinstry R, et al. Transient exposure of mammary tumors to PD184352 and UCN-01 causes tumor cell death *in vivo* and prolonged suppression of tumor regrowth. Cancer Biol Ther 2005;4:1275 – 84.

7. Allan LA, Morrice N, Brady S, Magee G, Pathak S, Clarke PR. Inhibition of caspase-9 through phosphorylation at Thr 125 by ERK MAPK. Nat Cell Biol 2003;5:647 – 54.

8. Mori M, Uchida M, Watanabe T, et al. Activation of extracellular signal-regulated kinases ERK1 and ERK2 induces Bcl-xL up-regulation via inhibition of caspase activities in erythropoietin signaling. J Cell Physiol 2003;195:290 – 7.

9. Ley R, Balmanno K, Hadfield K, Weston C, Cook SJ. Activation of the ERK1/2 signaling pathway promotes phosphorylation and proteasome-dependent degradation of the BH3-only protein, Bim. J Biol Chem 2003; 278:18811 – 6.

10. Wang YF, Jiang CC, Kiejda KA, Gillespie S, Zhang XD, Hersey P. Apoptosis induction in human melanoma cells by inhibition of MEK is caspase-independent and mediated by the Bcl-2 family members PUMA, Bim, and Mcl-1. Clin Cancer Res 2007;13:4934 – 42.

11. Qiao L, Han SI, Fang Y, et al. Bile acid regulation of C/EBPβ CREB, c-Jun function, via the extracellular signal-regulated kinase and c-Jun NH_2-terminal kinase pathways, modulates the apoptotic response of hepatocytes. Mol Cell Biol 2003;23:3052 – 66.

12. Allen LF, Sebolt-Leopold J, Meyer MB. CI-1040 (PD184352), a targeted signal transduction inhibitor of MEK (MAPKK). Semin Oncol 2003;30:105 – 16.

13. Davies BR, Logie A, McKay JS, et al. AZD6244 (ARRY-142886), a potent inhibitor of mitogen-activated protein kinase/extracellular signal-regulated kinase kinase 1/2 kinases: mechanism of action *in vivo*, pharmacokinetic/pharmacodynamic relationship, and potential for combination in preclinical models. Mol Cancer Ther 2007;6:2209 – 19.

14. Bagatell R, Whitesell L. Altered Hsp90 function in cancer: a unique therapeutic opportunity. Mol Cancer Ther 2004;3:1021 – 30.

15. Neckers L, Neckers K. Heat-shock protein 90 inhibitors as novel cancer chemotherapeutic agents. Expert Opin Emerg Drugs 2002;7: 277 – 88.

16. DeBoer C, Meulman PA, Wnuk RJ, Peterson DH. Geldanamycin, a new antibiotic. J Antibiot (Tokyo) 1970;23:442 – 7.

17. Isaacs JS, Xu W, Neckers L. Heat shock protein 90 as a molecular target for cancer therapeutics. Cancer Cell 2003;3:213 – 7.

18. Nimmanapalli R, O'Bryan E, Kuhn D, Yamaguchi H, Wang HG, Bhalla KN. Regulation of 17-AAG-induced apoptosis: role of Bcl-2, Bcl-XL, Bax downstream of 17-AAG-mediated down-regulation of Akt, Raf-1, and Src kinases. Blood 2003;102:269 – 75.

19. Stancato LF, Silverstein AM, Owens-Grillo JK, Chow YH, Jove R, Pratt WB. The hsp90-binding antibiotic geldanamycin decreases Raf levels and epidermal growth factor signaling without disrupting formation of signaling complexes or reducing the specific enzymatic activity of Raf kinase. J Biol Chem 1997;272:4013 – 20.

20. Nimmanapalli R, O'Bryan E, Bhalla K. Geldanamycin and its analogue 17-allylamino-17-demethoxygeldanamycin lowers Bcr-Abl levels and induces apoptosis and differentiation of Bcr-Abl-positive human leukemic blasts. Cancer Res 2001;61:1799 – 804.

21. Ramanathan RK, Trump DL, Eiseman JL, et al. Phase I pharmacokinetic-pharmacodynamic study of 17-(allylamino)-17-demethoxygeldanamycin (17AAG, NSC 330507), a novel inhibitor of heat shock protein 90, in patients with refractory advanced cancers. Clin Cancer Res 2005;11: 3385 – 91.

22. Lane D, Robert V, Grondin R, Rancourt C, Piche A. Malignant ascites protect against TRAIL-induced apoptosis by activating the PI3K/Akt pathway in human ovarian carcinoma cells. Int J Cancer 2007;121: 1227 – 37.

23. Georgakis GV, Li Y, Rassidakis GZ, Martinez-Valdez H, Medeiros LJ, Younes A. Inhibition of heat shock protein 90 function by 17-allylamino-17-demethoxy-geldanamycin in Hodgkin's lymphoma cells down-regulates Akt kinase, dephosphorylates extracellular signal-regulated kinase, and induces cell cycle arrest and cell death. Clin Cancer Res 2006;12:584 – 90.

24. Larribere L, Khaled M, Tartare-Deckert S, et al. PI3K mediates protection against TRAIL-induced apoptosis in primary human melanocytes. Cell Death Differ 2004;11:1084 – 91.

25. Grem JL, Morrison G, Guo XD, et al. Phase I and pharmacologic study of 17-(allylamino)-17-demethoxygeldanamycin in adult patients with solid tumors. J Clin Oncol 2005;23:1885 – 93.

26. Banerji U, O'Donnell A, Scurr M, et al. Phase I pharmacokinetic and pharmacodynamic study of 17-allylamino, 17-demethoxygeldanamycin in patients with advanced malignancies. J Clin Oncol 2005;23:4152 – 61.

27. Mitchell C, Park MA, Zhang G, et al. 17-Allylamino-17-demethoxygeldanamycin enhances the lethality of deoxycholic acid in primary rodent hepatocytes and established cell lines. Mol Cancer Ther 2007;6: 618 – 32.

28. Nguyen TK, Rahmani M, Gao N, et al. Synergistic interactions between DMAG and mitogen-activated protein kinase kinase 1/2 inhibitors in Bcr/abl + leukemia cells sensitive and resistant to imatinib mesylate. Clin Cancer Res 2006;12:2239 – 47.

29. Roth W, Reed JC. FLIP protein and TRAIL-induced apoptosis. Vitam Horm 2004;67:189 – 206.

30. Gupta S, Natarajan R, Payne SG, et al. Deoxycholic acid activates the c-Jun N-terminal kinase pathway via FAS receptor activation in primary hepatocytes. Role of acidic sphingomyelinase-mediated ceramide generation in FAS receptor activation. J Biol Chem 2004;279: 5821 – 8.

31. Qiao L, Studer E, Leach K, et al. Deoxycholic acid (DCA) causes ligand-independent activation of epidermal growth factor receptor (EGFR) and FAS receptor in primary hepatocytes: inhibition of EGFR/mitogen-activated protein kinase-signaling module enhances DCA-induced apoptosis. Mol Biol Cell 2001;12:2629 – 45.

32. Kamal A, Thao L, Sensintaffar J, et al. A high-affinity conformation of Hsp90 confers tumour selectivity on Hsp90 inhibitors. Nature 2003;425: 407 – 10.

33. Teufel A, Staib F, Kanzler S, Weinmann A, Schulze-Bergkamen H, Galle PR. Genetics of hepatocellular carcinoma. World J Gastroenterol 2007;13:2271 – 82.

34. Tannapfel A, Sommerer F, Benicke M, et al. Mutations of the BRAF gene in cholangiocarcinoma but not in hepatocellular carcinoma. Gut 2003;52:706 – 12.

35. Lee JW, Soung YH, Kim SY, et al. PIK3CA gene is frequently mutated in breast carcinomas and hepatocellular carcinomas. Oncogene 2005;24: 1477 – 80.

36. Hu TH, Huang CC, Lin PR, et al. Expression and prognostic role of tumor suppressor gene PTEN/MMAC1/TEP1 in hepatocellular carcinoma. Cancer 2003;97:1929 – 40.

37. Qiao L, Leach K, McKinstry R, et al. Hepatitis B virus X protein increases expression of p21(Cip-1/WAF1/MDA6) and p27(Kip-1) in primary mouse hepatocytes, leading to reduced cell cycle progression. Hepatology 2001;34:906 – 17.

38. Williams JS, Andrisani OM. The hepatitis B virus X protein targets the basic region-leucine zipper domain of CREB. Proc Natl Acad Sci U S A 1995;92:3819 – 23.

39. Wang WH, Gregori G, Hullinger RL, Andrisani OM. Sustained activation of p38 mitogen-activated protein kinase and c-Jun N-terminal kinase pathways by hepatitis B virus X protein mediates apoptosis via induction of Fas/FasL and tumor necrosis factor (TNF) receptor 1/TNF-α expression. Mol Cell Biol 2004;24:10352 – 65.

40. Rahmani M, Maynard-Davis E, Bauer C, Dent P, Grant S. Apoptosis induced by the kinase inhibitor Bay 43-9006 in human leukemia cells involves down-regulation of MCL-1 through inhibition of translation. J Biol Chem 2005;280:35217 – 27.

41. Lorusso PM, Adjei AA, Varterasian M, et al. Phase I and pharmacodynamic study of the oral MEK inhibitor CI-1040 in patients with advanced malignancies. J Clin Oncol 2005;23:5281 – 93.

42. Thompson N, Lyons J. Recent progress in targeting the Raf/MEK/ERK pathway with inhibitors in cancer drug discovery. Curr Opin Pharmacol 2005;5:350 – 6.

43. Rinehart J, Adjei AA, Lorusso PM, et al. Multi-center phase II study of the oral MEK inhibitor, CI-1040, in patients with advanced non-small-cell lung, breast, colon, and pancreatic cancer. J Clin Oncol 2004;22: 4456 – 62.

44. Dutton A, Young LS, Murray PG. The role of cellular FLICE inhibitory protein (c-FLIP) in the pathogenesis and treatment of cancer. Expert Opin Ther Targets 2006;10:27 – 35.

45. Koga F, Tsutsumi S, Neckers LM. Low dose geldanamycin inhibits hepatocyte growth factor and hypoxia-stimulated invasion of cancer cells. Cell Cycle 2007;6:1393 – 402.

46. Yang D, Yaguchi T, Yamamoto H, Nishizaki T. Intracellularly transported adenosine induces apoptosis in HuH-7 human hepatoma cells by downregulating c-FLIP expression causing caspase-3/-8 activation. Biochem Pharmacol 2007;73:1665 – 75.

47. Dey A, Cederbaum AI. Geldanamycin, an inhibitor of Hsp90 increases cytochrome *P*450 2E1 mediated toxicity in HepG2 cells through sustained activation of the p38MAPK pathway. Arch Biochem Biophys 2007;461: 275 – 86.

48. Fang Y, Han SI, Mitchell C, et al. Bile acids induce mitochondrial ROS, which promote activation of receptor tyrosine kinases and signaling pathways in rat hepatocytes. Hepatology 2004;40:961 – 71.

49. Huynh H, Soo KC, Chow PK, Tran E. Targeted inhibition of the extracellular signal-regulated kinase kinase pathway with AZD6244 (ARRY-142886) in the treatment of hepatocellular carcinoma. Mol Cancer Ther 2007;6:138 – 46.

Molecular Cancer Therapeutics

Mitogen-activated protein kinase kinase 1/2 inhibitors and 17-allylamino-17-demethoxygeldanamycin synergize to kill human gastrointestinal tumor cells *in vitro* via suppression of c-FLIP-s levels and activation of CD95

Margaret A. Park, Guo Zhang, Clint Mitchell, et al.

Mol Cancer Ther 2008;7:2633-2648.